

CoLLMLight: Cooperative Large Language Model Agents for Network-Wide Traffic Signal Control

Zirui Yuan

The Hong Kong University of Science
and Technology (Guangzhou)
zyuan779@connect.hkust-gz.edu.cn

Siqi Lai

The Hong Kong University of Science
and Technology (Guangzhou)
slai125@connect.hkust-gz.edu.cn

Hao Liu*

The Hong Kong University of Science
and Technology (Guangzhou)
liuh@ust.hk

Abstract

Traffic Signal Control (TSC) plays a critical role in urban traffic management by optimizing traffic flow and mitigating congestion. While Large Language Models (LLMs) have recently emerged as promising tools for TSC due to their exceptional problem-solving and generalization capabilities, existing approaches fail to address the essential need for inter-agent coordination, limiting their effectiveness in achieving network-wide optimization. To bridge this gap, we propose **CoLLMLight**, a cooperative LLM agent framework for TSC. Specifically, we first construct a structured spatiotemporal graph to capture real-time traffic dynamics and spatial relationships among neighboring intersections, enabling the LLM to reason about complex traffic interactions. Moreover, we introduce a complexity-aware reasoning mechanism that dynamically adapts reasoning depth based on real-time traffic conditions, ensuring optimal computational efficiency without sacrificing decision quality. Besides, we propose a fine-tuning strategy that leverages iterative simulation-driven data collection and environmental feedback to build a light-weight LLM tailored for cooperative TSC. Extensive experiments on both synthetic and real-world datasets demonstrate that CoLLMLight outperforms state-of-the-art methods in diverse traffic scenarios, showcasing its effectiveness, scalability, and robustness. Our code is available at <https://github.com/usail-hkust/CoLLMLight>.

Keywords

traffic signal control, large language model, multi-agent cooperation, intelligent transportation

ACM Reference Format:

Zirui Yuan, Siqi Lai, and Hao Liu. 2018. CoLLMLight: Cooperative Large Language Model Agents for Network-Wide Traffic Signal Control. In *Proceedings of Make sure to enter the correct conference title from your rights confirmation email (Conference acronym 'XX)*. ACM, New York, NY, USA, 14 pages. <https://doi.org/XXXXXXX.XXXXXXX>

1 Introduction

Traffic congestion has become a critical challenge, significantly affecting both society and the urban environment. With the rapid

acceleration of urban migration, city populations are expanding, further exacerbating this issue. Traffic Signal Control (TSC) is vital in optimizing traffic flow and improving road safety [27, 31, 38]. Over the past decades, numerous studies have explored both transportation-based and data-driven approaches to TSC. However, effectively managing traffic signals in complex and dynamic urban road networks remains a formidable challenge.

Transportation-based methods primarily rely on heuristic algorithms that dynamically adjust signals based on real-time lane-level traffic conditions [3, 9, 10, 13, 15, 20, 23]. However, these approaches often require extensive manual design and struggle to generalize across complex, dynamic traffic patterns [27]. In contrast, data-driven methods leverage reinforcement learning (RL) to learn optimal control policies through continuous environmental interactions, capturing multi-level embeddings of traffic dynamics [2, 12, 17, 25, 31]. To further enhance coordination across intersections and achieve road network-wide optimization, recent studies [4, 14, 26, 30, 34] integrate graph neural networks (GNNs) [1] to efficiently aggregate spatial information from neighboring intersections. These RL-based approaches have achieved state-of-the-art performance by leveraging collaborative traffic signal control. However, RL-based methods face significant generalization challenges, particularly in adapting to unseen or highly variable traffic conditions, due to their reliance on limited training data and data-centric optimization processes [11].

The advent of Large Language Models (LLMs) has introduced a paradigm shift across multiple domains, showcasing exceptional problem-solving and generalization capabilities. Recent studies have demonstrated their potential in TSC, highlighting their ability to tackle complex tasks with human-like reasoning [5, 11]. However, existing LLM-based approaches are limited by their focus on localized decision-making, neglecting the critical aspect of cross-intersection collaboration necessary for global traffic optimization. As illustrated in Figure 1(a), introducing neighborhood information significantly enhances the performance of both RL-based and LLM-based TSC approaches, emphasizing the importance of cross-intersection collaboration in effective traffic management. Despite this, enabling LLMs to reason about intricate traffic patterns across multiple neighboring intersections presents two key challenges.

The first challenge lies in enabling LLM agents to comprehend the intricate traffic interactions among neighboring intersections. This requires, first, identifying spatial relationships, such as lane connectivity and inter-dependencies between intersections. Second, the agents need to reason about dynamic traffic interactions, including real-time congestion propagation and queue spillbacks. A critical aspect is the ability to predict how their local decisions will influence not only the assigned intersection but also adjacent ones,

*Corresponding author

Permission to make digital or hard copies of all or part of this work for personal or classroom use is granted without fee provided that copies are not made or distributed for profit or commercial advantage and that copies bear this notice and the full citation on the first page. Copyrights for components of this work owned by others than the author(s) must be honored. Abstracting with credit is permitted. To copy otherwise, or republish, to post on servers or to redistribute to lists, requires prior specific permission and/or a fee. Request permissions from permissions@acm.org.
Conference acronym 'XX, Woodstock, NY

© 2018 Copyright held by the owner/author(s). Publication rights licensed to ACM.
ACM ISBN 978-1-4503-XXXX-X/2018/06
<https://doi.org/XXXXXXX.XXXXXXX>

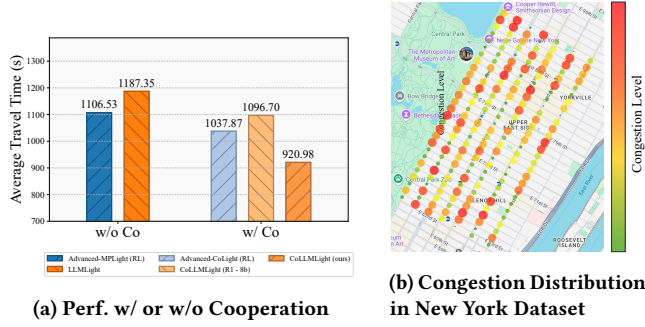


Figure 1: (a): Both RL-based and LLM-based methods can benefit from cross-intersection collaboration. (b): Congestion levels vary significantly across different locations.

ensuring that coordination leads to network-wide improvements. This presents a complex cooperation problem, where each agent must simultaneously model both spatiotemporal dependencies and anticipate cascading effects.

Achieving this complex coordination requires a nuanced reasoning process to ensure accurate decision-making. One approach to this is inference-time scaling [6, 22], which involves extending the length of the Chain-of-Thought (CoT) [29], allowing models to perform deeper, more structured reasoning. However, real-world traffic conditions vary significantly across locations, as illustrated in Figure 1(b). Some intersections experience light traffic with minimal vehicle presence, making signal optimization relatively straightforward. In contrast, heavily congested intersections require more sophisticated reasoning, as optimal signal selection depends on complex interactions with neighboring traffic flows. Applying the same reasoning depth to all intersections is inefficient: simpler cases do not benefit from extensive computation, while congested areas demand more nuanced analysis. A uniform approach not only wastes computational resources but is also impractical for real-time decision-making at scale. Thus, achieving a balance between computational efficiency and decision-making accuracy is another critical challenge.

To tackle these challenges, we propose CoLLMLight, a cooperative LLM agent framework tailored for TSC. To enable the LLM to comprehend intricate traffic interactions, we first collect real-time traffic state information from neighboring intersections over a recent time window. Then, a structured spatiotemporal graph is constructed to capture both spatial connectivity and temporal traffic dynamics. Leveraging this graph, the LLM predicts future traffic states under different signal configurations, evaluates their network-wide impacts, and selects the optimal signal to improve overall traffic conditions.

Furthermore, to ensure both efficiency and effectiveness, we introduce a complexity-aware reasoning mechanism that classifies decision-making complexity into three levels—ranging from lightly to highly congested intersections—and adapts reasoning strategies accordingly. The agent dynamically adjusts its reasoning depth based on real-time traffic conditions, optimizing computational resource allocation without sacrificing decision quality.

To further enhance performance, we propose a fine-tuning strategy for building a lightweight LLM tailored for cooperative traffic signal control. Through an iterative simulation-driven data collection process, we synthesize task-specific reasoning chains to improve traffic pattern comprehension. We then employ GPT-4o to evaluate simulation outputs and generate high-quality pseudo labels for reasoning complexity identification, future traffic state prediction, and signal selection. Additionally, a policy refinement process with environmental feedback iteratively improves decision-making, ensuring maximized network-wide traffic efficiency.

Our contributions are summarized as follows: 1) We propose **CoLLMLight**, a cooperative LLM agent framework for network-wide traffic signal control. To our knowledge, this is the first work to integrate LLM cooperation into TSC. 2) We design a complexity-aware reasoning mechanism that dynamically adapts reasoning modes based on real-time traffic conditions, ensuring an optimal balance between computational efficiency and performance. 3) We propose an LLM fine-tuning method for cooperative TSC, which learns traffic dynamics through iterative simulation and environmental feedback, leading to significant improvements in decision-making and efficiency. 4) Extensive evaluations on both synthetic and real-world datasets validate the effectiveness and superiority of CoLLMLight in diverse traffic scenarios.

2 Problem Statement

In this section, we introduce key concepts related to traffic signal control and the formal problem statement. A more detailed illustration of the most used setting of the intersection, lanes, and signal phases are in Appendix A.1

DEFINITION 1 (ROAD NETWORK). *The road network is a directed graph connected by intersections \mathcal{V} and lanes \mathcal{L} . Lanes can be categorized into three types: 1) go-through lanes (\mathcal{L}_{go}), 2) left-turn lanes (\mathcal{L}_{left}), 3) right-turn lanes (\mathcal{L}_{right}). These lanes are interconnected with their neighboring intersections.*

DEFINITION 2 (TRAFFIC SIGNALS). *At each signal-switching time step, the agent assigned to the intersection selects a signal from the predefined signal set $\mathcal{A} = \{a_1, \dots, a_m\}$. The traffic signal is represented as $a = \text{set}(\mathcal{L}_{allow})$, where \mathcal{L}_{allow} is a group of allowed-to-go lanes without conflicting movements (i.e., a green light for \mathcal{L}_{allow} and a red light for others).*

PROBLEM 1 (MULTI-AGENT LLM FOR NETWORK-WIDE TRAFFIC SIGNAL CONTROL). *Consider a road network with multiple intersections, each intersection is controlled by an LLM agent with a control policy π . At each signal-switching timestep t , each agent receives: 1) traffic observations from both assigned and neighboring intersections \mathcal{O}_t ; 2) spatial relations among intersections \mathcal{G} ; 3) historical traffic interactions \mathcal{T}_t ; 4) relative task descriptions \mathcal{D} . Based on these inputs, the agent reasons the optimal traffic signal action a_t from the action space \mathcal{A} , with the goals of maximizing the network-wide traffic efficiency:*

$$a_t = \pi([\mathcal{O}_t, \mathcal{G}, \mathcal{T}_t], \mathcal{D}, \mathcal{A}). \quad (1)$$

3 Cooperative LLM Agent Framework

We present the framework of CoLLMLight in Figure 2, including: 1) *Spatiotemporal-aware cooperative decision-making*: It enables the

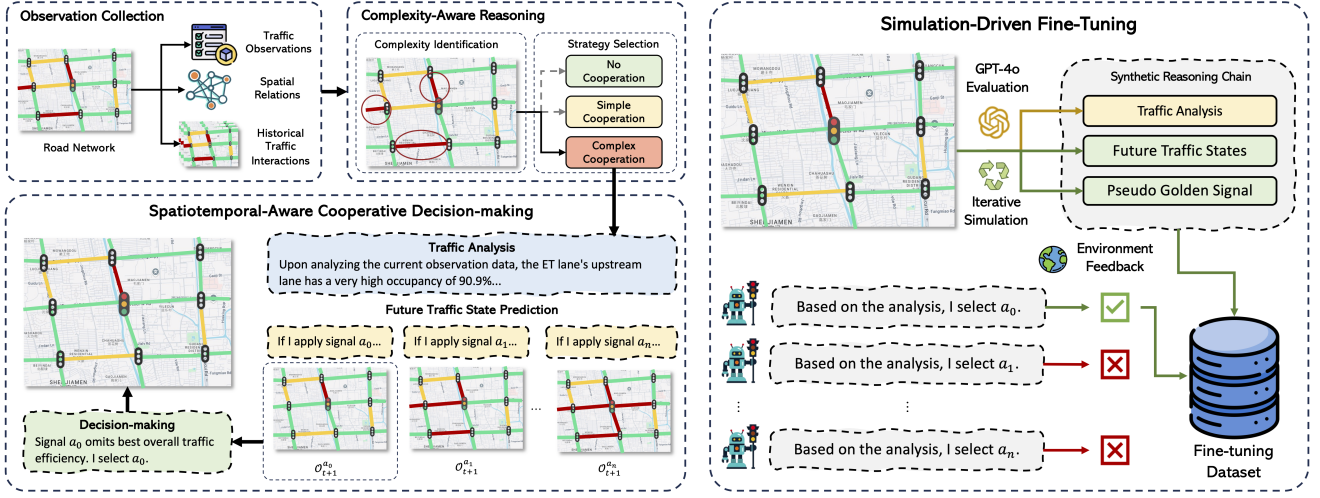


Figure 2: The overview of CoLLMLight framework.

LLM to understand and leverage spatiotemporal information, allowing it to capture intricate traffic interactions and make accurate, coordinated decisions. 2) *Complexity-aware reasoning*: By evaluating the current traffic conditions, it dynamically selects the most appropriate reasoning mode, ensuring that computational resources are efficiently allocated without sacrificing decision quality. 3) *Simulation-driven fine-tuning*: Through iterative simulation, this component generates task-specific data that is used to fine-tune the LLM, thereby enhancing its decision-making accuracy and efficiency in cooperative TSC scenarios.

3.1 Spatiotemporal-Aware Cooperative Decision-Making

Complex traffic coordination scenarios require the LLM agent to infer traffic states not only at its assigned intersection but also at neighboring intersections. This inference is based on the spatial dependencies between intersections and the temporal dynamics of congestion propagation across the network. We propose a spatiotemporal-aware cooperative decision-making mechanism that enables the LLM agent to effectively integrate both spatial and temporal information, thereby optimizing traffic flow across the road network.

3.1.1 Observation Collection. We begin by formulating lane-level observations at the current timestep t as:

$$\mathbf{o}_t = [n^{\text{queue}}, n^{\text{move}}, \tau, \rho], \quad (2)$$

where n^{queue} represents the number of vehicles in the queue, n^{move} denotes the number of vehicles currently moving, τ indicates the average waiting time, and $\rho \in [0, 1]$ reflects the traffic occupancy of the lane. These lane-level observations are then aggregated to construct both local and neighboring observations at the assigned and nearby intersections as $\mathcal{O}_t = \{\mathbf{o}_l | l \in \mathcal{L}\}$, where \mathcal{L} represents the set of lanes connected to the agent's assigned intersection and its neighboring intersections.

3.1.2 Spatiotemporal Modeling. In the road network topology, lanes exhibit directional connectivity across intersections. To represent these spatial relationships, we construct a directed subgraph for each intersection, denoted as $\mathcal{G} = (\mathcal{V}, \mathcal{L})$, where \mathcal{V} is the set of intersections (including both the assigned and neighboring intersections), and \mathcal{L} denotes the set of adjacent lanes connecting these intersections.

To capture the temporal pattern of congestion propagation, we collect historical traffic interactions over fixed time windows Δt , which include past traffic observations with corresponding activated signal configurations:

$$\mathcal{T}_t = \{(\mathcal{O}_{t_i}, \mathbf{a}_{t_i}) | t - \Delta t < t_i < t\}, \quad (3)$$

where \mathbf{a}_{t_i} represents the signal configurations at both the assigned and neighboring intersections at time t_i .

3.1.3 Cooperative Decision-Making. To enable the LLM to understand our constructed observations and spatiotemporal features, we generate a human-readable prompt that combines current traffic observations \mathcal{O}_t , the spatial relation graph \mathcal{G} , historical traffic interactions \mathcal{T}_t , and task instructions \mathcal{D} (e.g., preventing vehicle release into congested downstream lanes or dynamically adjusting lane usage in response to upstream congestion). To scale the chain-of-thought (CoT) process, the LLM follows a detailed three-step decision-making process: First, it analyzes the current traffic conditions at both the assigned and neighboring intersections. Next, it predicts neighboring future traffic states under different signal configurations. Finally, based on these predictions, it selects the signal configuration that is most likely to optimize network-wide traffic flow. Formally, this process is represented as:

$$\mathbf{X} = \text{Prompt}(\mathcal{O}_t, \mathcal{G}, \mathcal{T}_t, \mathcal{D}), \quad (4)$$

$$\mathbf{Y}_{\text{ana}}, \{\hat{\mathcal{O}}_{t+1}^a | a \in \mathcal{A}\}, \hat{a} = f_{\text{LLM}}(\mathbf{X}), \quad (5)$$

where \mathbf{X} is the verbalized LLM input, \mathbf{Y}_{ana} is the analysis on the current traffic condition, $\hat{\mathcal{O}}_{t+1}^a$ represents the predicted traffic states for each signal configuration a at the next timestep, and \hat{a} is the estimated optimal signal.

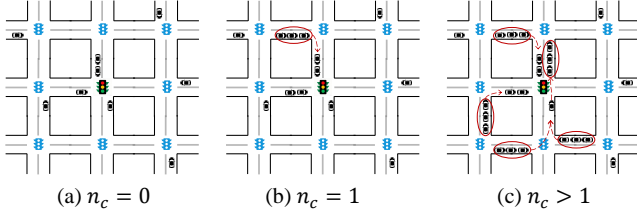


Figure 3: An illustration of traffic scenarios with varying coordination complexity. Critical lanes are circled in red. (a) $n_c = 0$ (No cooperation): Signals can be determined locally. (b) $n_c = 1$ (Simple cooperation): The agent needs to consider the interaction with one critical lane. (c) $n_c > 1$ (Complex Cooperation): The agent needs to consider interactions with multiple critical lanes.

3.2 Complexity-Aware Reasoning

While a spatiotemporal-aware decision-making process significantly improves accuracy by capturing complex traffic dependencies among intersections, it often incurs substantial inference time due to the need for generating long token sequences. Applying such computationally intensive reasoning uniformly across all scenarios can be impractical, as it may compromise real-time responsiveness in dynamic traffic environments. To address this, we propose a complexity-aware reasoning approach, enabling the LLM to automatically assess the complexity of decision-making at each intersection and adaptively select the most cost-efficient reasoning strategy without sacrificing performance.

We first classify the reasoning complexity at an intersection based on a congestion risk coefficient n_c , which is the number of critical neighboring lanes that are either congested or at risk of congestion. As illustrated in Figure 3:

1) $n_c = 0$ (No Cooperation): When no critical neighboring lanes are congested, the intersection operates independently, requiring no complex cooperative decision-making for signal optimization. In this case, both traffic condition analysis and future traffic state prediction are omitted:

$$\hat{a} = f_{\text{LLM}}^{\text{no-coop}}(\mathbf{X}). \quad (6)$$

2) $n_c = 1$ (Simple Cooperation): When exactly one neighboring lane exhibits high traffic occupancy, the agent must analyze local spatiotemporal dependencies between adjacent intersections. However, since the congestion is limited to a single neighboring lane, the future traffic state prediction process is excluded.

$$\mathbf{Y}_{\text{ana}}, \hat{a} = f_{\text{LLM}}^{\text{simple}}(\mathbf{X}). \quad (7)$$

3) $n_c > 1$ (Complex Cooperation): When multiple neighboring lanes are highly congested, the agent must account for more extensive spatiotemporal dependencies, including multi-hop effects across intersections. In this scenario, the complete cooperative decision-making process is applied:

$$\mathbf{Y}_{\text{ana}}, \{\hat{O}_{t+1}^a | a \in \mathcal{A}\}, \hat{a} = f_{\text{LLM}}^{\text{complex}}(\mathbf{X}). \quad (8)$$

We instruct the LLM to identify the congestion risk coefficient n_c and dynamically select the corresponding reasoning strategy.

3.3 Simulation-Driven Fine-Tuning

To further enhance the reasoning capability of LLM in spatiotemporal-aware cooperation, we propose a fine-tuning method that incorporates iterative simulation-based data collection. Our approach consists of two stages: 1) reasoning chain optimization and 2) policy refinement with environmental feedback.

3.3.1 Reasoning Chain Optimization. We first utilize the traffic simulator CityFlow [36] with a synthesized traffic flow dataset to generate diverse traffic scenarios spanning various congestion levels. We follow the required LLM outputs specified in Section 3.1.3, which include congestion risk n_c , traffic analysis \mathbf{Y}_{ana} , future traffic states $\{\hat{O}_{t+1}^a | a \in \mathcal{A}\}$, and the optimal signal configuration a^* for activation.

To derive congestion risk and traffic analysis, we utilize GPT-4o to generate a structured summary of traffic conditions at both the assigned intersection and its neighboring intersections:

$$n_c, \mathbf{Y}_{\text{ana}} = f_{\text{GPT-4o}}(O_t). \quad (9)$$

To estimate future traffic states, we roll out the simulation under different signal configurations and collect the corresponding next-step traffic states:

$$\{\hat{O}_{t+1}^a | a \in \mathcal{A}\} = \{f_{\text{sim}}(O_t, a) | a \in \mathcal{A}\}, \quad (10)$$

where f_{sim} denotes the simulator's state transition function. To determine the pseudo-golden signal a^* , we simulate various signal actions and evaluate their impact on traffic flow. Specifically, we select the signal configuration that minimizes the total number of queued vehicles over a five-timestep horizon in the neighboring intersections:

$$a^* = \underset{a \in \mathcal{A}}{\operatorname{argmin}} f_{\text{queue}}(O_t, a), \quad (11)$$

where f_{queue} represents the simulator's queue length measurement function. This pseudo-golden signal serves as an optimal supervisory signal for training.

Given the required LLM outputs for each reasoning strategy employed, we synthesize the corresponding reasoning chain by a structured summarization of GPT-4o. To optimize the LLM, we apply supervised fine-tuning, minimizing the negative log-likelihood of generating the target reasoning chain:

$$\text{loss} = - \sum_{w=1}^{|Y|} \log P_{\pi}(y_w | \mathbf{X}, \mathbf{Y}_{<w}), \quad (12)$$

where \mathbf{Y} is the synthesized reasoning chain, $P_{\pi}(y_w | \mathbf{X}, \mathbf{Y}_{<w})$ represents the probability of generating the token y_w given the prompt \mathbf{X} and the preceding tokens in the reasoning chain $\mathbf{Y}_{<w}$.

3.3.2 Refinement with Environment Feedback. After optimizing the reasoning chain, the LLM can effectively follow our constructed reasoning process. However, its decision-making remains suboptimal due to potential hallucinations in traffic conditions and misinterpretations of spatiotemporal dependencies. To address this, we propose an iterative refinement process incorporating environmental feedback for further optimization.

Specifically, we simulate different traffic signal configurations based on the LLM's decision-making and evaluate their effectiveness using an environment feedback function, Q . A higher feedback value indicates a more favorable signal configuration under

Table 1: Statistics of datasets.

Flow dataset	Structure	# of vehicles	Intersection Connectivity Index				
			Max	Q_3	Std	Mean	Min
New York 1	28×7	11058	2.513	0.894	0.479	0.518	0.017
New York 2		16337	3.666	1.325	0.706	0.767	0.025
Jinan 1	3×4	6295	0.717	0.654	0.059	0.617	0.509
Jinan 2		4365	0.502	0.464	0.035	0.438	0.385
Jinan 3		5494	0.622	0.573	0.048	0.544	0.48
Hangzhou 1	4×4	2983	0.318	0.217	0.057	0.18	0.097
Hangzhou 2		6984	0.815	0.492	0.17	0.413	0.217
Syn-Train	4×4	8000	3.463	1.785	0.979	1.38	0.028

the given traffic conditions. We then identify the reasoning chain associated with the signal configuration that yields the highest environmental feedback, which will be designated as a golden pseudo reasoning chain for further fine-tuning:

$$\{Y|\hat{a} = \operatorname{argmax}_{a \in \mathcal{A}} Q(O_t, a)\}_{t=0}^T, \quad (13)$$

where T represents the time window over which environmental feedback is collected. The environment feedback function Q is defined as the inverse of the overall queue length at neighboring intersections after a five-timestep duration, ensuring that lower congestion is rewarded with higher feedback values.

4 Experiments

We perform extensive experiments to assess the framework’s effectiveness, efficiency, and generalizability in various urban traffic scenarios, addressing the following research questions:

- **RQ1:** How does CoLLMLight’s performance compare to traditional TSC methods and general LLMs?
- **RQ2:** What impacts do CoLLMLight’s components have on its performance and efficiency?
- **RQ3:** How do neighboring information and temporal dynamics influence the framework’s performance and computational efficiency?

4.1 Experimental Setup

4.1.1 Datasets. Our experiments were conducted on seven real-world [27] and one synthetic traffic flow dataset. Comprehensive statistics for these datasets are presented in Table 1. Syn-Train is a dataset that we synthesized. In our experiment, all learning-based methods (RL-based, LLMLight, CoLLMLight) are trained on the Syn-Train and tested for their zero-shot performance in real-world datasets.

- **Jinan:** A dataset from the Dongfeng sub-district in Jinan, China, consisting of 12 intersections. The dataset includes three traffic flow datasets captured across different time periods, with each intersection featuring two 400-meter roads (east-west) and two 800-meter roads (north-south).
- **Hangzhou:** A dataset from the Gudang sub-district in Hangzhou, China, comprising 16 intersections and two traffic flow datasets across different temporal periods, with each intersection featuring two 800-meter roads (east-west) and two 600-meter roads (north-south).

- **New York:** Collected in Manhattan’s Upper East Side using taxi trip data, this extensive dataset encompasses 196 intersections, with each road measuring 300 meters. It includes two large-scale traffic flow datasets from different periods.
- **Syn-Train:** A synthetic dataset comprising 16 intersections, with each road segment measuring 300 meters. This dataset serves as the primary training data for learning-based traffic signal control methods in our experimental framework.

To compare the differences in coordination complexity across these datasets, we define the *Intersection Connectivity Index* as follows:

DEFINITION 3 (INTERSECTION CONNECTIVITY INDEX (ICI)). *The Intersection Connectivity Index quantifies an intersection’s correlation with its adjacent intersections. An intersection with a high ICI that fails to coordinate with its neighbors may lead to congestion. The ICI for intersection \mathcal{V}_i can be calculated as follows:*

$$ICI = \sum_{\mathcal{V}_j \in \mathcal{N}(\mathcal{V}_i)} \left(\frac{n_{ij}v}{d_{ij}} \right), \quad (14)$$

where $\mathcal{N}(\mathcal{V}_i)$ represents the set of neighboring intersections connected to \mathcal{V}_i , v is the average vehicle speed, d_{ij} is the road length between \mathcal{V}_i and \mathcal{V}_j , and n_{ij} is the average number of vehicles passing between \mathcal{V}_i and \mathcal{V}_j per 30 seconds.

As observed in Table 1, New York’s ICI exhibits significantly higher maximum and upper quartile (Q_3) values compared to Jinan and Hangzhou. This suggests that the New York traffic network demands more sophisticated traffic signal cooperation strategies than others.

4.1.2 Environment Settings. We utilize CityFlow [36], a widely used open-source simulator, to perform our experiments. We employ four signal phases as control actions: ETWT (east-west through), ELWL (east-west left-turn), NTST (north-south through), and NLSL (north-south left-turn). Each traffic flow dataset simulates an hour. In the simulation, right-turn movements are allowed at all times. The green signal phase lasts for thirty seconds, followed by a three-second yellow phase and a two-second all-red phase [11, 26, 37].

4.1.3 Compared Methods. We compare our proposed method with two conventional transportation methods: FixedTime [10] and MaxPressure [23]; six RL-based approaches: MPLight [2], AttendLight [17], PressLight [25], CoLight [26], Efficient-CoLight [32], and Advanced-CoLight [37]; and a SOTA LLM-based method: LLM-Light [11]. Additionally, we assess the performance of general LLMs integrated within our CoLLMLight framework, including Llama 3.1 (8B and 70B), Qwen 2.5 (70B), and the Deepseek-R1 distilled models (R1-8B and R1-32B).

4.1.4 Evaluation Metrics. We adopt *Average Travel Time* (ATT) and *Average Waiting Time* (AWT) [11, 28, 37] as evaluation metrics to evaluate the performance of various traffic signal control methods. Specifically, ATT quantifies the average duration required for vehicles to travel from their origins to their respective destinations. AWT quantifies the average queuing time experienced by vehicles at each intersection within the road network.

Table 2: Zero-Shot Performance Comparison across Different Datasets (Lower Values Indicate Better Performance). Performance Rankings: best results in boldface, second-best results with double underline, and third-best results with single underline. The lower part of the table shows the performance of various LLMs using the CoLLMLight agent framework.

Models	New York 1		New York 2		Jinan 1		Jinan 2		Jinan 3		Hangzhou 1		Hangzhou 2	
	ATT	AWT	ATT	AWT	ATT	AWT	ATT	AWT	ATT	AWT	ATT	AWT	ATT	AWT
FixedTime	1535.65	290.12	1771.74	428.71	481.79	70.98	441.19	66.71	450.11	69.19	616.01	73.98	486.76	72.79
MaxPressure	1223.26	153.27	1566.77	255.46	282.57	44.53	273.19	38.24	265.75	40.19	325.32	49.60	347.74	70.57
MPLight	1492.15	262.23	1711.04	364.61	461.76	73.35	482.21	84.57	429.01	67.60	496.15	64.67	440.63	71.47
AttendLight	1267.74	292.75	1755.28	496.78	392.68	69.05	310.22	63.38	337.39	67.33	327.17	72.85	348.06	68.60
PressLight	1687.16	508.38	1894.04	489.66	376.88	87.34	410.09	139.17	367.82	93.93	599.95	259.18	539.62	317.85
CoLight	1443.28	280.61	1704.67	392.05	516.87	93.93	474.35	79.98	491.63	86.16	526.63	74.61	479.84	88.78
Efficient - CoLight	1266.04	281.32	1645.69	437.33	765.04	532.01	844.80	489.91	846.29	558.33	874.53	466.77	672.38	408.90
Advanced - CoLight	1037.87	185.49	1428.90	359.79	414.25	138.18	392.89	144.74	441.79	176.21	427.99	235.86	410.79	154.06
LLMLight - 8B	1187.35	143.06	1599.44	388.74	274.97	43.98	268.57	40.45	<u>259.49</u>	40.12	311.99	39.54	332.46	61.16
Llama3.1 - 8B	1153.74	148.92	1446.12	<u>224.50</u>	331.32	85.21	310.81	75.21	305.55	79.31	343.20	82.00	353.80	88.27
Deepseek R1 - 8B	1096.70	<u>120.51</u>	1454.74	325.28	285.94	40.85	272.83	39.51	266.74	38.92	314.19	44.75	336.20	55.06
Deepseek R1 - 32B	<u>1011.01</u>	<u>114.80</u>	<u>1256.11</u>	<u>202.76</u>	<u>277.36</u>	35.13	<u>266.98</u>	33.78	<u>260.46</u>	<u>34.53</u>	<u>305.81</u>	34.18	323.71	39.01
Llama3.1 - 70B	<u>1023.15</u>	143.44	1400.00	284.74	293.09	45.56	274.78	39.09	270.74	40.21	314.08	41.98	<u>332.06</u>	53.65
Qwen2.5 - 72B	1128.54	177.94	<u>1392.48</u>	244.49	279.10	35.66	267.34	<u>33.81</u>	261.30	34.34	<u>304.57</u>	<u>34.28</u>	332.43	46.82
CoLLMLight - 8B	920.98	85.90	1218.94	170.13	<u>276.41</u>	<u>35.25</u>	266.89	<u>34.50</u>	258.89	<u>34.47</u>	303.77	<u>34.72</u>	<u>326.02</u>	<u>44.12</u>

4.2 Implementation Details

We conducted our experiments on Linux servers that were equipped with two A800 GPUs. All RL methods are trained with consistent hyperparameters: a learning rate of 1×10^{-3} , a replay buffer size of 12,000, a sample size of 3,000, and a hidden size of 20. For LLMs, the temperature parameter is set to 0.1. We perform LoRA fine-tuning on Llama 3.1 (8B) to obtain LLMLight and CoLLMLight, maintaining LoRA settings with a rank of 8 and a scaling factor α of 16, along with a learning rate of 1×10^{-4} . During the reasoning tuning stage, we construct 2,802 trajectories and sample an additional 552 trajectories from Syn-Train during the policy refinement stage.

4.3 Comparative Performance (RQ1)

In the first experiment, all learning-based methods were trained on the synthetic traffic flow dataset, Syn-Train, and evaluated on seven real-world traffic flow datasets to assess their zero-shot performance. The results are presented in Table 2.

Specifically, CoLLMLight consistently achieves SOTA or comparable performance against all baselines, demonstrating superior generalization and cooperation capabilities. This indicates that CoLLMLight can effectively adapt its learned policies to various traffic scenarios. Among the previous methods, MaxPressure demonstrates superior generalization capabilities compared to most RL-based approaches, which often struggle to adapt their performance to new scenarios due to their data-centric nature. While LLMLight excels in Jinan 1, it struggles with complex coordination in New York, revealing the limitations of its localized decision-making.

In our evaluation of generalist LLMs within the CoLLMLight framework, Deepseek R1-32B exhibits performance comparable to CoLLMLight-8B in Jinan and Hangzhou. However, in the New York dataset, which presents higher coordination complexity, CoLLMLight-8B outperforms all baselines, achieving a 25.17% reduction in AWT for New York 1 and a 16.09% reduction for New York 2 compared to the second-best performance.

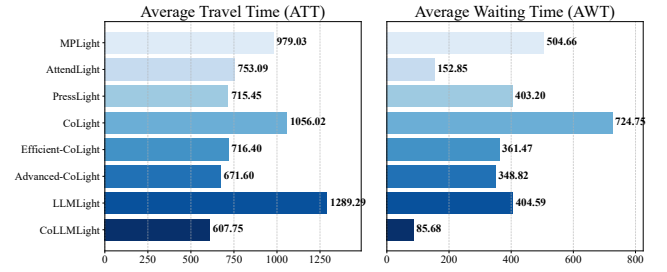


Figure 4: Comparative Performance of Learning-based Methods at Syn-Train

We also report the performance of learning-based methods on the Syn-Train dataset in Figure 4. CoLLMLight outperforms all other methods in this dataset due to its effective policy refinement, which enhances its cooperative abilities within the traffic environment, leading to superior TSC performance. In contrast, LLMLight demonstrates poor performance due to its policy not considering coordination among intersections, which is critical at Syn-Train. Among RL-based methods, Advanced-CoLight shows the best learning performance in the Syn-Train dataset; however, it struggles to transfer this performance to real-world datasets. In contrast, CoLLMLight generalizes the policy learned from Syn-Train, achieving effective coordination and demonstrating its robustness across different traffic scenarios. Additionally, we compare DeepSeek-R1 (671B) and O1mini on the New York 1 dataset, as detailed in the Appendix A.4. The results show that CoLLMLight outperforms the SOTA LLMs within complex coordination scenarios.

4.4 Ablation Study (RQ2)

4.4.1 Ablation of Reasoning Strategy. The complexity-aware reasoning mechanism balances performance and efficiency by intelligently identifying current cooperation complexity and switching



Figure 5: Performance and efficiency of various variants across four datasets. Methods positioned towards the lower left (\swarrow) exhibit superior performance (\downarrow) while incurring lower time costs (\leftarrow).

Table 3: Abalation Tests of Optimization Stages

Model	Jinan			Hangzhou		New York	
	1	2	3	1	2	1	2
w/o Both	331.32	310.81	305.55	343.20	353.80	1153.74	1446.12
w/o RO	312.39	294.47	291.66	338.39	351.85	1167.37	1500.65
w/o PR	278.35	267.73	261.03	304.52	327.92	1085.88	1368.03
Ours	276.41	266.89	258.89	303.77	326.02	920.98	1218.94

among three reasoning strategies: $f_{LLM}^{no-coop}$, f_{LLM}^{simple} , and $f_{LLM}^{complex}$. These strategies are denoted as NC, SR, and CR. This section evaluates the impact of these reasoning strategies by comparing the performance and total inference time across various variants.

(1) **Single Reasoning Strategy.** These variants do not incorporate complexity identification and rely solely on a single reasoning strategy to determine the optimal traffic signal.

(2) **Two Reasoning Strategies (w/o NC, w/o SR, w/o CR).** These variants integrate two reasoning strategies. For instance, w/o NC indicates the CoLLMLight without $f_{LLM}^{no-coop}$, but with f_{LLM}^{simple} and $f_{LLM}^{complex}$. The experimental results are presented in Figure 5.

Among these three variants, w/o SR demonstrates strong cost-effectiveness in the New York dataset but fails in the Jinan and Hangzhou datasets due to its low efficiency in simple cooperation scenarios. In contrast, our method integrates all three strategies to address the cooperation problem more flexibly. By utilizing reasoning strategies tailored to different traffic scenarios, our method outperforms the complex reasoning in most datasets while achieving significant efficiency improvements.

4.4.2 Ablation of Optimization Stages. This ablation study evaluates the effectiveness of our training stages by comparing our model against three variants: (1) **w/o Both:** the base Llama3.1 8b model,

which serves as the initial baseline without any specialized training; (2) **w/o RO:** a variant that omits reasoning chain optimization, which directly applies the base Llama3.1 8b model to interact with the environment and collect trajectories for policy refinement; (3) **w/o PR:** a variant that has conducted reasoning chain optimization but discards policy refinement. The comparative results are shown in Table 3.

The experimental results show that the ablation of any components leads to a drop in performance, highlighting the critical roles of reasoning chain optimization and policy refinement in enhancing our model’s performance. Without these optimizations, the base model struggles to produce effective traffic signal control trajectories, especially in complex urban traffic scenarios, such as those in New York. Moreover, if we directly apply refinement using environmental feedback, performance in New York may actually decline, as indicated by the results of the w/o RO variant. This decline is due to the lack of a fundamental reasoning process that is essential for effective control strategies in various urban environments.

The results of the w/o PR variant indicate the model’s fundamental reasoning capabilities for cooperative traffic signal control has been activated, showing strong performance in smaller traffic networks such as Jinan and Hangzhou, where traffic patterns are relatively simpler. However, without further refining its policy with environmental feedback, the model still struggles in more complex environments like New York, which features intricate traffic dynamics and higher coordination requirements. By further fine-tuning the model’s policy, our method demonstrates substantial performance improvements, particularly in the New York dataset. These gains illustrate that feedback refinement effectively enhances the model’s ability to generalize across diverse and challenging traffic environments, bridging the gap between learned imitation and optimal control strategies.

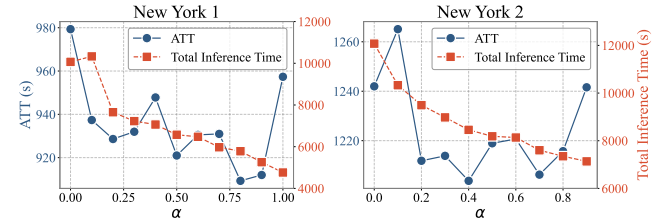


Figure 6: Average Travel Time and Total Inference Time with varying communication threshold α .

4.5 Analysis of Spatiotemporal Information (RQ3)

In this section, we analyze the impact of the spatiotemporal information processed by our agent by conducting a sensitivity analysis on two key hyperparameters (the communication threshold α and the historical window size Δt) to adjust neighboring information and temporal information, respectively.

4.5.1 Analysis of Neighboring Information. In our observation collection process, only neighboring lanes with occupancy above the threshold α are aggregated. A larger α results in less neighboring

information being considered. We vary α from 0 to 1 while keeping $\Delta t = 5$, and the results are reported in Figure 6.

Specifically, when we set $\alpha = 0$, the intersection must consider all neighboring lanes, leading to longer processing times and a higher likelihood of errors. As α increases, unimportant lanes with low occupancy are filtered out, reducing inference time and allowing the model to focus on the critical lanes that may contribute to congestion, thereby improving performance. However, if α becomes too high, critical lanes may also be disregarded, resulting in decreased performance. In our main experiments, we set $\alpha = 0.5$.

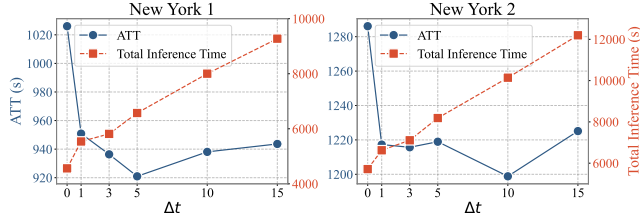


Figure 7: Average Travel Time and Total Inference Time with varying historical window size Δt .

4.5.2 Analysis of Historical Information Δt . The value of Δt determines the amount of historical information available to the agent. We vary Δt within the range $[0, 1, 3, 5, 10, 15]$ while keeping $\alpha = 0.5$. The results are reported in Figure 7.

Specifically, when $\Delta t = 0$, the agent does not consider any historical information in its decision-making, resulting in the lowest performance across all datasets. Once the agent considers a timestep of information, the ATT shows a significant decrease, highlighting the importance of historical information for effective traffic signal control. However, the computational overhead increases linearly with Δt due to the larger input text processed by the LLM agent. Importantly, performance does not consistently improve with an increased historical window size. We observe performance degradation when Δt exceeds 5 or 10 timesteps. This decline can be attributed to the increased complexity and potential noise introduced by longer input contexts. To balance performance and efficiency, we set $\Delta t = 5$ for our main experiments.

5 Related Work

5.1 Traffic Signal Control

Traffic signal control presents a significant challenge within intelligent transportation systems, with methodological approaches evolving across traditional transportation methods, RL-based methods, and LLM TSC agents. Traditional strategies include FixedTime [10], which relies on predetermined cycle lengths and phase allocations, and Maxpressure [23], which is designed to mitigate over-saturation by minimizing the difference in total queue lengths between incoming and outgoing traffic flows. RL-based methods have transformed the field through innovative neural architectures and advanced feature representations. Notable approaches include FRAP [39], which introduced a dynamic phase-level interaction network; CoLight [26], leveraging graph attention networks [24] for inter-intersection

coordination; CosLight [21], utilizing MLP to construct the collaborator matrix among all intersections. Concurrently, researchers have focused on developing more sophisticated traffic state representations. PressLight [25] pioneered pressure-based state representations to enhance traffic management, Efficient-XLight [32] introduced efficient pressure, and Advanced-XLight [37] further advanced performance by combining it with effective vehicle count.

Recently, emerging LLMs have demonstrated transformative potential, as seen in frameworks like LLMLight [11], which showcases exceptional generalization by mimicking human-like reasoning processes. However, current LLM-based TSC agents ignore the coordination among intersections, which is crucial for alleviating traffic congestion.

5.2 Multi-Agent Cooperation of Large Language Models

Recently, LLM-based multi-agent systems have achieved considerable progress across various domains [7], demonstrating remarkable performance in software development [8, 19], multi-robot systems [16, 35], and societal simulation [18]. These innovative systems leverage multiple autonomous agents to collaboratively engage in complex planning, nuanced discussions, and sophisticated decision-making, effectively mimicking the intricate cooperative dynamics of human group interactions. For instance, MetaGPT [8] embeds human workflow processes into language model agents, utilizing an assembly line strategy that assigns specialized roles to different agents to facilitate seamless cooperation. CoMAL [33] introduces a collaboration module that enables autonomous vehicles to collectively discuss and strategize, dynamically allocating roles to optimize collaborative performance.

However, many multi-agent LLM frameworks rely on iterative inter-agent communication, requiring multiple LLM calls for discussions and consensus-building, which limits their ability to provide the real-time responsiveness essential for traffic signal control. In contrast, CoLLMLight is an efficient cooperative agent that independently analyzes the dynamics of its collaborators, considers their interests, and makes decisions aimed at optimizing global traffic.

6 Conclusion

This paper introduces CoLLMLight, a cooperative LLM agent framework specifically designed for network-wide traffic signal control. To effectively address the complexities of traffic interactions and foster cooperation among intersections, we model the spatiotemporal information that LLM agent can receive in the traffic environment and propose a Spatiotemporal-Aware Cooperative Decision-Making approach to comprehensively analyze current traffic conditions, predict future states under various signal configurations, evaluate their network-wide impacts, and select optimal signals to enhance overall traffic flow. To promote efficiency, we introduce a Complexity-Aware Reasoning mechanism that classifies traffic scenario complexity into three distinct levels and integrates two additional efficient decision-making strategies for simpler cooperative scenarios. Additionally, we propose a Simulation-Driven Fine-Tuning approach to optimize our agent's reasoning chain and refine its policy through interaction with the environment. Extensive experiments conducted on both synthetic and real-world datasets

validate the superior performance of our framework, demonstrating its capability to effectively manage complex urban traffic scenarios with remarkable efficiency. In the future, we plan to investigate a hierarchical asynchronous Multi-Agent LLM framework for traffic signal control, aimed at guiding the real-time decision-making of intersection agents through regional-level planning.

References

- [1] Wendelin Böhmer, Vitaly Kurin, and Shimon Whiteson. 2020. Deep coordination graphs. In *International Conference on Machine Learning*. PMLR, 980–991.
- [2] Chacha Chen, Hua Wei, Nan Xu, Guanjie Zheng, Ming Yang, Yuanhao Xiong, Kai Xu, and Zhenhui Li. 2020. Toward a thousand lights: Decentralized deep reinforcement learning for large-scale traffic signal control. In *Proceedings of the AAAI conference on artificial intelligence*, Vol. 34. 3414–3421.
- [3] Seung-Bae Cools, Carlos Gershenson, and Bart D'Hooghe. 2013. Self-organizing traffic lights: A realistic simulation. *Advances in applied self-organizing systems* (2013), 45–55.
- [4] François-Xavier Devailly, Denis Larocque, and Laurent Charlin. 2021. IG-RL: Inductive graph reinforcement learning for massive-scale traffic signal control. *IEEE Transactions on Intelligent Transportation Systems* 23, 7 (2021), 7496–7507.
- [5] Jie Feng, Jun Zhang, Junbo Yan, Xin Zhang, Tianjian Ouyang, Tianhui Liu, Yuwei Du, Siqi Guo, and Yong Li. 2024. CityBench: Evaluating the Capabilities of Large Language Model as World Model. *arXiv preprint arXiv:2406.13945* (2024).
- [6] Daya Guo, Dejian Yang, Haowei Zhang, Junxiao Song, Ruoyu Zhang, Runxin Xu, Qihao Zhu, Shirong Ma, Peiyi Wang, Xiao Bi, et al. 2025. Deepseek-r1: Incentivizing reasoning capability in llms via reinforcement learning. *arXiv preprint arXiv:2501.12948* (2025).
- [7] Taicheng Guo, Xiuying Chen, Yaqi Wang, Ruidi Chang, Shichao Pei, Nitesh V. Chawla, Olaf Wiest, and Xiangliang Zhang. 2024. Large Language Model Based Multi-agents: A Survey of Progress and Challenges. In *Proceedings of the Thirty-Third International Joint Conference on Artificial Intelligence, IJCAI-24*, Kate Larson (Ed.). International Joint Conferences on Artificial Intelligence Organization, 8048–8057. doi:10.24963/ijcai.2024/890 Survey Track.
- [8] Sirui Hong, Mingchen Zhuge, Jonathan Chen, Xiawu Zheng, Yuheng Cheng, Jinlin Wang, Ceyao Zhang, Zili Wang, Steven Ka Shing Yau, Zijuan Lin, et al. 2024. MetaGPT: Meta Programming for A Multi-Agent Collaborative Framework. In *The Twelfth International Conference on Learning Representations*.
- [9] PB Hunt, DI Robertson, RD Bretherton, and M Cr Royle. 1982. The SCOOT on-line traffic signal optimisation technique. *Traffic Engineering & Control* 23, 4 (1982).
- [10] Peter Koonce et al. 2008. *Traffic signal timing manual*. Technical Report. United States. Federal Highway Administration.
- [11] Siqi Lai, Zhao Xu, Weijia Zhang, Hao Liu, and Hui Xiong. 2023. Large language models as traffic signal control agents: Capacity and opportunity. *arXiv preprint arXiv:2312.16044* (2023).
- [12] Enming Liang, Zicheng Su, Chilin Fang, and Renxin Zhong. 2022. Oam: An option-action reinforcement learning framework for universal multi-intersection control. In *Proceedings of the AAAI Conference on Artificial Intelligence*, Vol. 36. 4550–4558.
- [13] John DC Little, Mark D Kelson, and Nathan H Gartner. 1981. MAXBAND: A versatile program for setting signals on arteries and triangular networks. (1981).
- [14] Yican Lou, Jia Wu, and Yunchuan Ran. 2022. Meta-reinforcement learning for multiple traffic signals control. In *Proceedings of the 31st ACM International Conference on Information & Knowledge Management*. 4264–4268.
- [15] P Lowrie. 1990. Scats-a traffic responsive method of controlling urban traffic. *Sales information brochure published by Roads & Traffic Authority, Sydney, Australia* (1990).
- [16] Zhao Mandi, Shreeya Jain, and Shuran Song. 2024. Roco: Dialectic multi-robot collaboration with large language models. In *2024 IEEE International Conference on Robotics and Automation (ICRA)*. IEEE, 286–299.
- [17] Afshin Oroojlooy, Mohammadreza Nazari, Davood Hajinezhad, and Jorge Silva. 2020. Attendlight: Universal attention-based reinforcement learning model for traffic signal control. *Advances in Neural Information Processing Systems* 33 (2020), 4079–4090.
- [18] Joon Sung Park, Joseph O'Brien, Carrie Jun Cai, Meredith Ringel Morris, Percy Liang, and Michael S Bernstein. 2023. Generative agents: Interactive simulacra of human behavior. In *Proceedings of the 36th annual acm symposium on user interface software and technology*. 1–22.
- [19] Chen Qian, Wei Liu, Hongzhang Liu, Nuo Chen, Yufan Dang, Jiahao Li, Cheng Yang, Weize Chen, Yusheng Su, Xin Cong, et al. 2024. Chatdev: Communicative agents for software development. In *Proceedings of the 62nd Annual Meeting of the Association for Computational Linguistics (Volume 1: Long Papers)*. 15174–15186.
- [20] Roger P Roess. 2004. Traffic Engineering.
- [21] Jingqing Ruan, Ziyue Li, Hua Wei, Haoyuan Jiang, Jiaming Lu, Xuantang Xiong, Hanguo Mao, and Rui Zhao. 2024. Coslight: Co-optimizing collaborator selection and decision-making to enhance traffic signal control. In *Proceedings of the 30th ACM SIGKDD Conference on Knowledge Discovery and Data Mining*. 2500–2511.
- [22] Charlie Snell, Jaehoon Lee, Kelvin Xu, and Aviral Kumar. 2024. Scaling llm test-time compute optimally can be more effective than scaling model parameters. *arXiv preprint arXiv:2408.03314* (2024).
- [23] Pravin Varaiya. 2013. Max pressure control of a network of signalized intersections. *Transportation Research Part C: Emerging Technologies* 36 (2013), 177–195.
- [24] Petar Veličković, Guillem Cucurull, Arantxa Casanova, Adriana Romero, Pietro Lio, and Yoshua Bengio. 2017. Graph attention networks. *arXiv preprint arXiv:1710.10903* (2017).
- [25] Hua Wei, Chacha Chen, Guanjie Zheng, Kan Wu, Vikash Gayah, Kai Xu, and Zhenhui Li. 2019. Presslight: Learning max pressure control to coordinate traffic signals in arterial network. In *Proceedings of the 25th ACM SIGKDD international conference on knowledge discovery & data mining*. 1290–1298.
- [26] Hua Wei, Nan Xu, Huichu Zhang, Guanjie Zheng, Xinshi Zang, Chacha Chen, Weinan Zhang, Yanmin Zhu, Kai Xu, and Zhenhui Li. 2019. Colight: Learning network-level cooperation for traffic signal control. In *Proceedings of the 28th ACM international conference on information and knowledge management*. 1913–1922.
- [27] Hua Wei, Guanjie Zheng, Vikash Gayah, and Zhenhui Li. 2019. A survey on traffic signal control methods. *arXiv preprint arXiv:1904.08117* (2019).
- [28] Hua Wei, Guanjie Zheng, Vikash Gayah, and Zhenhui Li. 2021. Recent advances in reinforcement learning for traffic signal control: A survey of models and evaluation. *ACM SIGKDD Explorations Newsletter* 22, 2 (2021), 12–18.
- [29] Jason Wei, Xuezhi Wang, Dale Schuurmans, Maarten Bosma, Fei Xia, Ed Chi, Quoc V Le, Denny Zhou, et al. 2022. Chain-of-thought prompting elicits reasoning in large language models. *Advances in neural information processing systems* 35 (2022), 24824–24837.
- [30] Libing Wu, Min Wang, Dan Wu, and Jia Wu. 2021. Dynstgat: Dynamic spatial-temporal graph attention network for traffic signal control. In *Proceedings of the 30th ACM international conference on information & knowledge management*. 2150–2159.
- [31] Qiang Wu, Mingyuan Li, Jun Shen, Linyuan Lü, Bo Du, and Ke Zhang. 2023. Transformerlight: A novel sequence modeling based traffic signaling mechanism via gated transformer. In *Proceedings of the 29th ACM SIGKDD Conference on Knowledge Discovery and Data Mining*. 2639–2647.
- [32] Qiang Wu, Liang Zhang, Jun Shen, Linyuan Lü, Bo Du, and Jianqing Wu. 2021. Efficient pressure: Improving efficiency for signalized intersections. *arXiv preprint arXiv:2112.02336* (2021).
- [33] Huaiyuan Yao, Longchao Da, Vishnu Nandam, Justin Turnau, Zhiwei Liu, Linsey Pang, and Hua Wei. 2024. CoMAL: Collaborative Multi-Agent Large Language Models for Mixed-Autonomy Traffic. *arXiv preprint arXiv:2410.14368* (2024).
- [34] Zhengxu Yu, Shuxian Liang, Long Wei, Zhongming Jin, Jianqiang Huang, Deng Cai, Xiaofei He, and Xian-Sheng Hua. 2021. MaCAR: Urban traffic light control via active multi-agent communication and action rectification. In *Proceedings of the Twenty-Ninth International Conference on Artificial Intelligence*. 2491–2497.
- [35] Hongxin Zhang, Weihua Du, Jiaming Shan, Qinhong Zhou, Yilun Du, Joshua B. Tenenbaum, Tianmin Shu, and Chuang Gan. 2024. Building Cooperative Embodied Agents Modularly with Large Language Models. In *The Twelfth International Conference on Learning Representations*. <https://openreview.net/forum?id=EnXJfQqy0K>
- [36] Huichu Zhang, Siyuan Feng, Chang Liu, Yaoyao Ding, Yichen Zhu, Zihan Zhou, Weinan Zhang, Yong Yu, Haiming Jin, and Zhenhui Li. 2019. Cityflow: A multi-agent reinforcement learning environment for large scale city traffic scenario. In *The world wide web conference*. 3620–3624.
- [37] Liang Zhang, Qiang Wu, Jun Shen, Linyuan Lü, Bo Du, and Jianqing Wu. 2022. Expression might be enough: representing pressure and demand for reinforcement learning based traffic signal control. In *International Conference on Machine Learning*. PMLR, 26645–26654.
- [38] Weijia Zhang, Le Zhang, Jindong Han, Hao Liu, Yanjie Fu, Jingbo Zhou, Yu Mei, and Hui Xiong. 2024. Irregular Traffic Time Series Forecasting Based on Asynchronous Spatio-Temporal Graph Convolutional Networks. In *Proceedings of the 30th ACM SIGKDD Conference on Knowledge Discovery and Data Mining*. 4302–4313.
- [39] Guanjie Zheng, Yuanhao Xiong, Xinshi Zang, Jie Feng, Hua Wei, Huichu Zhang, Yong Li, Kai Xu, and Zhenhui Li. 2019. Learning phase competition for traffic signal control. In *Proceedings of the 28th ACM international conference on information and knowledge management*. 1963–1972.

A Appendix

A.1 Settings of Traffic Signal Control

We present the most used settings in Figure 8.

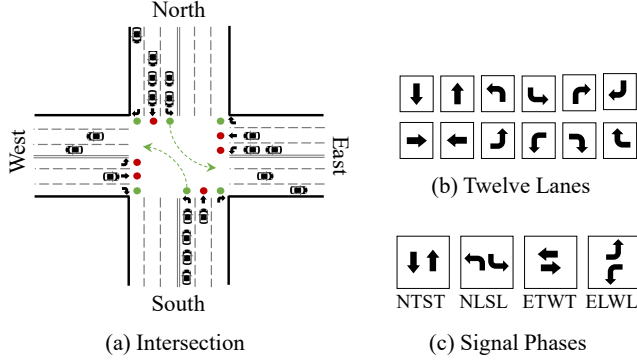


Figure 8: An illustration of intersections, lanes, and signal phases. The signal phases include ETWT (east-west through movement), ELWL (left-turn from east and west), NTST (north-south through movement), and NLSL (left-turn from north and south)

A.2 Prompt Template and Decision Making Process

We present our prompt template in Figures 9 and 10, and the decision-making process in Figures 11 and 12.

A.3 Compared Methods

- **FixedTime** [10]: A traditional signal control method using static, predefined cycle lengths and phase times.
- **MaxPressure** [23]: A SOTA transportation method selecting signal phases based on queue length pressure between upstream and downstream intersections.
- **MPLight** [2]: It utilizes pressure as both observation and reward, based on the FRAP.
- **AttendLight** [17]: It uses attention mechanisms to predict phase transitions and construct observation features.
- **PressLight** [25]: Applies Deep Reinforcement Learning (DRL) to optimize intersection pressure.
- **CoLight** [26]: Employs graph attention network (GAT) for inter-intersection communication.
- **Efficient-CoLight** [32]: Enhances CoLight by integrating efficient pressure observations.
- **Advanced-CoLight** [37]: A SOTA MARL-based method that enhances CoLight by integrating advanced traffic state features, including pressure and effective running vehicles.
- **LLMLight** [11]: A SOTA LLM TSC agent that employs a reasoning process mimicking human-like intuition to optimize traffic management.

A.4 Performance Comparison with DeepSeek R1-671B and O1-mini

We present the performance comparison results of CoLLMLight against the SOTA LLMs, DeepSeek R1-671B, and O1-mini, in Tables 5 and 4, respectively.

For DeepSeek R1-671B, we conducted an experiment using the New York 1 dataset, selecting the 10% most congested intersections to be controlled by the LLM agent, and tested its performance over a simulation time span of 1200 seconds. For O1-mini, we evaluated its performance in a complete setting, controlling all 196 intersections in the New York 1 dataset and simulating traffic for 3600 seconds. The results further demonstrate the superior performance of CoLLMLight.

Table 4: Performance Comparison between R1 and CoLLMLight, in a setting of 10% controlled by LLM Agents and 1200 seconds simulation.

Model	AWT	ATT
Deepseek R1-671B	97.148	846.587
CoLLMLight-8B	70.144	834.433

Table 5: Performance Comparison between O1mini and CoLLMLight, in a setting of 100% controlled by LLM Agents and 3600 seconds simulation.

Model	AWT	ATT
O1mini	95.20	986.91
CoLLMLight-8B	85.90	920.98

Background Context

An intersection has 12 lanes: [NL, NT, NR, SL, ST, SR, EL, ET, ER, WL, WT, WR]. Each lane is labeled by direction and movement: N for north, S for south, E for east, W for west, L for left turn, T for through, and R for right turn. For instance, ET stands for the East Through lane, where traffic moves straight ahead from east to west. WL is the West Left-turn lane, where traffic turns left from west to south. Right turns are always allowed. There are four signal options: [ETWT, NTST, ELWL, NLSL]. For example, ETWT indicates the release of both the ET and WT lanes. The signal phase duration is set to thirty seconds.

Note:

For each Lane X, when considering activating it, keep these in mind:

- NEVER let the occupancy of X's downstream lanes be close to 100% at any risk, as it will cause severe congestion.
- If the upstream or downstream information of X isn't mentioned, it means that they are in a good state with low occupancy.
- You MUST consider how much the occupancy of X's downstream lanes will increase upon releasing lane X.
- You MUST delay the release of X if its downstream has a high occupancy rate.
- If there are many high-occupancy lanes upstream of X and X's occupancy is not low, you MUST consider releasing X so as to help upstream lanes release.

- You can't keep a lane waiting for too long. You MUST release the lane with excessive waiting time when the downstream condition allows.

Data

Historical ObservationTimestep: 48

Signal: ELWL

Lane	Cars Input	Cars Output	Queued Cars Change	Queued Cars	Moving Cars Change	Moving Cars	Average Waiting Time Change (mins)	Average Waiting Time (mins)	Occupancy Change (%)	Occupancy (%)
ST	9	0	2.0	7	9	0.35	27.27	33.33		
SL	0	0	1.0	0	0.5	2.83	0.0	3.03		
ET	1	0	0.0	1	1	0.0	3.03	3.03		
WL	1	5	-5.0	0	1	-1.07	0.0	-12.12	3.03	
ET's upstream lane (32, NT)	1	10	-16.0	18.0	7	9	0.2	0.69	-27.27	81.82

.....

Timestep: 52

Signal: NTST

Lane	Cars Input	Cars Output	Queued Cars Change	Queued Cars	Moving Cars Change	Moving Cars	Average Waiting Time Change (mins)	Average Waiting Time (mins)	Occupancy Change (%)	Occupancy (%)	
ST	1	9	-4.0	0	4	5	-0.42	0.0	-24.24	15.15	
SL	0	0	1.0	0	0.5	4.83	0.0	3.03			
ET	1	0	2.0	2	0	0.09	0.09	3.03	6.06		
WL	3	0	3.0	6	0	2	0.13	0.59	9.09	24.24	
ST's downstream lane (4, ST)	7	8	-14.0	4	0	13	13	-0.71	0.07	-3.03	51.52
ET's upstream lane (32, NT)	10	0	19.0	19	0	9	11	0.24	0.24	30.3	90.91
WL's downstream lane (4, ST)	7	8	-14.0	4	0	13	13	-0.71	0.07	-3.03	51.52

Current Observation

Timestep: 53

Intersection Lanes - Controlled by You:

Lane	Queued Cars	Moving Cars	Average Waiting Time (mins)	Occupancy	
ST	0	0	5	0.0	15.2%
SL	1	0	4.8	3.0%	
ET	2	0	0.1	6.1%	
WL	6	0	2	0.6	24.2%

['NT', 'NL', 'EL', 'WT'] are empty.

Nearby Upstream and Downstream Lanes - Controlled by Other Intersections near You:

We use (inter_id, lane) to represent these lanes. For instance, (1, 'NL') represents the NL lane at Intersection 1.

Relation	Queued Cars	Moving Cars	Average Waiting Time (mins)	Occupancy	
Your ST's downstream lane (4, 'ST')	4	0	13	0.1	51.5%
Your ET's upstream lane (32, 'NT')	19	0	11	0.2	90.9%
Your WL's downstream lane (4, 'ST')	4	0	13	0.1	51.5%

Signal Priority (local)

This rank only consider your own intersection, and assume the downstream allow the release.

Rank	Signal	Waiting Time Reduction
1	ELWL	7.6 mins
2	NLSL	5.3 mins
3	NTST	2.5 mins
4	ETWT	1.2 mins

Figure 9: Prompt Template Part 1

Task:

Your task consists of two phases:

Phase 1: Coordination Scenario Classification

1. Analyze the data in `\Current Observation\` and classify the intersection into one of three coordination scenarios:

- **No-Coordination**: No upstream or downstream coordination needs.
- **Simple-Coordination**: One upstream or downstream lanes require coordination with low traffic complexity.
- **Complex-Coordination**: High traffic complexity with significant congestion multiple upstream or downstream lanes.

Phase 2: Signal Selection Strategy

Based on the identified coordination scenario, select the appropriate signal using the following strategies:

a. No-Coordination

- Directly select the highest-ranked priority signal, as there are no external coordination considerations.

b. Simple-Coordination

- Focus on the `\Current Observation\` data.
- Keep the `\Notes\` in mind, compare each signal, and select the optimal one based on traffic conditions.

c. Complex-Coordination

Conduct a comprehensive analysis and select the optimal signal by following these steps:

1. **Current Traffic Data Analysis**: Rank lanes based on queued cars and waiting times.
2. **Upstream Analysis**: Assess the conditions of nearby and long-distance upstream lanes for each lane.
3. **Downstream Analysis**: Assess the conditions of nearby and long-distance downstream lanes for each lane.
4. **Signal Consequence Prediction**: Utilize `\Historical Observation\` data for inferring the consequences of each signal.
5. **Signal Comparison**: Systematically compare the effects of each signal option.
6. **Decision Making**: Make a decision on the optimal signal to activate.

Requirement:

Please provide a JSON formatted output as follows:

```
```json
{
 \phase1\: {
 \thought_process\: \Your thought process text description\,
 \answer\: \NO\ | \Simple\ | \Complex\
 },
 \phase2\: {
 \thought_process\: \Your thought process text description\,
 \answer\: \ETWT\ | \NTST\ | \ELWL\ | \NLSL\
 }
}
```
```

Figure 10: Prompt Template Part 2


```

```json
{
 \"phase1\": {
 \"thought_process\": \"Upon analyzing the current observation data, we need to assess the occupancy levels of both upstream and downstream lanes. The ET lane's upstream lane (32, 'NT') has a very high occupancy of 90.9%, which indicates a significant congestion issue. This requires careful coordination to prevent further congestion. The ST lane's downstream lane (4, 'ST') has an occupancy of 51.5%, which is moderate but not critical. The WL lane shares the same downstream lane (4, 'ST') with the ST lane, also at 51.5% occupancy. Given the high occupancy of the ET lane's upstream and the moderate occupancy of the ST and WL lanes' downstream, this situation requires coordination to manage the traffic flow effectively. Therefore, the intersection is classified under 'Complex-Coordination' due to the high traffic complexity and significant congestion in the upstream lane.\",
 \"answer\": \"Complex\"
 },
 \"phase2\": {
 \"thought_process\": \"1. **Current Traffic Data Analysis**:\\nBased on the current traffic data, the lanes can be ranked as follows: WL has the highest number of queued cars with 6 and an average waiting time of 0.6 minutes. ET has 2 queued cars with a waiting time of 0.1 minutes. SL has 1 queued car with a waiting time of 4.8 minutes, indicating it has been waiting for a significant amount of time despite having only one car. ST has no queued cars and a waiting time of 0.0 minutes, indicating smooth flow.\\n\\n2. **Upstream Analysis**:\\nFor the ET lane, the upstream lane (32, 'NT') is heavily congested with 19 queued cars and an occupancy of 90.9%. This suggests a high demand for releasing the ET lane to alleviate upstream congestion. The WL lane does not have any upstream congestion issues mentioned, indicating it is not a priority for release based on upstream conditions.\\n\\n3. **Downstream Analysis**:\\nThe ST lane's downstream (4, 'ST') has an occupancy of 51.5%, which is moderate but not critical. This suggests that releasing the ST lane would not cause downstream congestion. The WL lane shares the same downstream as ST, also at 51.5% occupancy, indicating that releasing WL would not cause downstream issues. The ET lane does not have any downstream congestion issues mentioned, suggesting it can be released without causing downstream congestion.\\n\\n4. **Signal Consequence Prediction**\\n**If activate ETWT**:\\n| Lane| Cars Input| Cars Output| Queued Cars Change| Queued Cars| Moving Cars Change| Moving Cars| Average Waiting Time Change (mins)| Average Waiting Time (mins)| Occupancy Change (%)| Occupancy (%)|\\n| ST| 0| 0| 5.0| 5.0| -5| 0| 0.38| 0.38| 0.0| 15.15|\\n| SL| 0| 0| 0.0| 1.0| 0| 0| 0.5| 5.33| 0.0| 3.03|\\n| ET| 0| 2| -2.0| 0.0| 0| 0| -0.09| 0.0| -6.06| 0.0|\\n| WL| 0| 0| 2.0| 8.0| -2| 0| 0.39| 0.98| 0.0| 24.24|\\n| ST's downstream lane (4, ST)| 7| 8| -14.0| 4.0| 13| 13| -0.71| 0.07| -3.03| 51.52|\\n| ET's upstream lane (32, NT)| 9| 0| 19.0| 19.0| -10| 1| 0.24| 0.24| 27.27| 90.91|\\n| WL's downstream lane (4, ST)| 7| 8| -14.0| 4.0| 13| 13| -0.71| 0.07| -3.03| 51.52|\\n\\n
 }
}

```

Figure 11: Decision Making Process 1

```

If activate NTST:\
|Lane|Cars Input|Cars Output|Queued Cars Change|Queued Cars|Moving Cars Change|Moving Cars|Average Waiting
Time Change (mins)|Average Waiting Time (mins)|Occupancy Change (%)|Occupancy (%)|\
|ST|0|5|0.0|0.0|-5|0|0.0|0.0|-15.15|0.0|\
|SL|0|0|0.0|1.0|0|0|0.5|5.33|0.0|3.03|\
|ET|0|0|0.0|2.0|0|0|0.5|0.59|0.0|6.06|\
|WL|0|0|2.0|8.0|-2|0|0.39|0.98|0.0|24.24|\
|ST's downstream lane (4, ST)|7|8|-14.0|4.0|13|13|-0.71|0.07|-3.03|51.52|\
|ET's upstream lane (32, NT)|9|0|19.0|19.0|-10|1|0.24|0.24|27.27|90.91|\
|WL's downstream lane (4, ST)|7|8|-14.0|4.0|13|13|-0.71|0.07|-3.03|51.52|\
\
If activate ELWL:\
|Lane|Cars Input|Cars Output|Queued Cars Change|Queued Cars|Moving Cars Change|Moving Cars|Average Waiting
Time Change (mins)|Average Waiting Time (mins)|Occupancy Change (%)|Occupancy (%)|\
|ST|0|0|5.0|5.0|-5|0|0.38|0.38|0.0|15.15|\
|SL|0|0|0.0|1.0|0|0|0.5|5.33|0.0|3.03|\
|ET|0|0|0.0|2.0|0|0|0.5|0.59|0.0|6.06|\
|WL|0|8|-6.0|0.0|-2|0|-0.59|0.0|-24.24|0.0|\
|ST's downstream lane (4, ST)|7|8|-14.0|4.0|13|13|-0.71|0.07|-3.03|51.52|\
|ET's upstream lane (32, NT)|9|0|19.0|19.0|-10|1|0.24|0.24|27.27|90.91|\
|WL's downstream lane (4, ST)|7|8|-14.0|4.0|13|13|-0.71|0.07|-3.03|51.52|\
\
If activate NLSL:\
|Lane|Cars Input|Cars Output|Queued Cars Change|Queued Cars|Moving Cars Change|Moving Cars|Average Waiting
Time Change (mins)|Average Waiting Time (mins)|Occupancy Change (%)|Occupancy (%)|\
|ST|0|0|5.0|5.0|-5|0|0.38|0.38|0.0|15.15|\
|SL|0|1|-1.0|0.0|0|0|-4.83|0.0|-3.03|0.0|\
|ET|0|0|0.0|2.0|0|0|0.5|0.59|0.0|6.06|\
|WL|0|0|2.0|8.0|-2|0|0.39|0.98|0.0|24.24|\
|ST's downstream lane (4, ST)|7|8|-14.0|4.0|13|13|-0.71|0.07|-3.03|51.52|\
|ET's upstream lane (32, NT)|9|0|19.0|19.0|-10|1|0.24|0.24|27.27|90.91|\
|WL's downstream lane (4, ST)|7|8|-14.0|4.0|13|13|-0.71|0.07|-3.03|51.52|\
\
5. **Signal Comparison**:\
Upon analyzing the signal options, we observe the following: Activating ETWT will clear the ET lane, which is crucial due
to the high occupancy of its upstream lane (NT) at 90.9%. This will also help reduce the waiting time for the ET lane.
However, it will increase the queued cars in the WL lane, which is already at a moderate occupancy. Activating NTST will
clear the ST lane, which has no queued cars and is not a priority. It will also not address the high occupancy of the ET
lane's upstream. Activating ELWL will clear the WL lane, which has the highest number of queued cars, and reduce its
occupancy significantly. However, it will not address the high occupancy of the ET lane's upstream. Activating NLSL will
clear the SL lane, which has been waiting for a significant time, but it will not address the high occupancy of the ET
lane's upstream. Given the current conditions, the ETWT option is optimal as it addresses the critical upstream
congestion of the ET lane and prevents further congestion in the NT lane.\
\
6. **Decision Making**:\
ETWT",
 \ "answer": \ "ETWT"
}
}
...

```

Figure 12: Decision Making Process 2